Universality in few-body systems: from few-atoms to few-nucleons

A Kievsky[1], M Gattobigio[2], E Garrido[3]

[1]Istituto Nazionale di Fisica Nucleare, Largo B. Pontecorvo 3, 56127 Pisa, Italy
[2]Université de Nice-Sophia Antipolis, Institut Non-Linéaire de Nice, CNRS, 1361 route des Lucioles, 06560 Valbonne, France
[3]Instituto de Estructura de la Materia, CSIC, Serrano 123, E-28006 Madrid, Spain

E-mail: kievsky@pi.infn.it

Abstract. Some aspects of universal properties are discussed in few-atom as well as in few-nucleon systems. When the two-body scattering length a is large the three-body system presents some peculiar characteristics such as the Efimov effect. In the present contribution, the zero-range theory deduced by V. Efimov is compared to results obtained using potential models. Accordingly range corrections are introduced. These corrections appear as a shift in the variable $\kappa_* a$ with κ_* the three-body parameter. The three-boson spectrum, atom-dimer scattering and the recombination rate at threshold are analyzed using the finite-range theory proposed. In the case of nuclear systems, $n-d$ scattering is discussed using the universal formula derived by Efimov. Furthermore, the spectrum up to $N = 6$ is discussed using the central Volkov potential.

1. Introduction

The scattering of two particles at very low energy E shows universal behavior encoded on the effective range function in that regime

$$k \cot \delta = -\frac{1}{a} + \frac{1}{2} r_s k^2 \ , \tag{1}$$

where $k^2 = E/(\hbar^2/m)$, δ is the phase shift and r_s is the effective range of the interaction. In fact, systems interacting differently but having equal values of the scattering length a and effective range r_s share the same low energy behavior. Two different limits can be studied that produce interesting effects in the three-body system. The first one is the scaling limit: the range, r_0, of the potential goes to zero. In this limit the two-body system presents a continuous scale invariance (CSI): the low energy observables depend on a single parameter, the two-body scattering length a. For example the s-wave phase shift reads $k \cot \delta = -1/a$ and, for positive values of a, a two-body bound state appears (called dimer) with binding energy $E_2 = \hbar^2/ma^2$. In this context a appears as a control parameter. As it has been demonstrated by Thomas in 1935 [1], the three-body system collapses in this limit (this effect is known as the Thomas collapse). Using a variational argument Thomas showed that the three-body ground state energy scales as $\hbar^2/mr_0^2$ producing a system unbound from below as $r_0 \to 0$. Remarkably, this collapse is independent of the magnitude of the two-body binding energy.

The second limit, which is subject of intense investigations, is the unitary limit. In this limit $|a| >> r_0$ and, in the case of positive and large values of a, a shallow dimer appears with binding

energy $E_2 \approx \hbar^2/ma^2$. As pointed out by V. Efimov in 1970 and subsequent papers [2, 3], when $a >> r_0$ the three-boson system presents a new class of universal behavior. The spectrum of three interacting bosons results from a geometric series: $E^{n+1}/E^n \to \mathrm{e}^{-2\pi/s_0}$ with $s_0 \approx 1.00624$ a universal constant. What is observed, introducing the three-body hyperradial variable ρ, is that a very extended hyperradial potential is generated which, as $\rho \to \infty$, goes to $\hbar^2/ma^2$. In the limit $a \to \infty$ the hyperradial potential goes to zero as $1/\rho^2$ supporting an infinite number of bound states. The short range physics can be implemented as a boundary condition at short distances (of the order of the interaction range r_0) and, as n increases, the universal spectrum results. More specifically when $a >> r_0$ a continuous scale invariance appears in the two-body system while, in the three-body system, it is broken to a discrete scale invariance (DSI).

The DSI imposes strong constrains on the observables. In addition to the geometric spectrum already mentioned in the case of three-boson bound states, the atom-dimer scattering length a_{AD} has the following functional form deduced by Efimov [4]

$$a_{AD}/a = d_1 + d_2 \tan[s_0 \ln(\kappa_* a) + d_3] \,, \tag{2}$$

where d_1, d_2, d_3 are universal constants and κ_* is the three-body parameter that fixes the energy scale at the unitary limit (see Ref. [5] for details).

For collisions below the dimer breakup threshold the DSI imposes the following universal form for the effective range function

$$ka \cot \delta_{AD} = c_1(ka) + c_2(ka) \cot[s_0 \ln(a\kappa_*) + \phi(ka)] \,, \tag{3}$$

with δ_{AD} the atom-dimer phase-shift and c_1, c_2, ϕ universal functions depending on the product ka, where $k^2 = (4/3)E/(\hbar^2/m)$, being E the center of mass energy of the process. As $k \to 0$, $ka \cot \delta_{AD} \to -1/a_{AD}$ and at $k = 0$ the constants d_1, d_2, d_3 and $c_1(0), c_2(0), \phi(0)$ are related by simple trigonometric equalities. A parametrization of the functions c_1, c_2, ϕ can be found in Ref. [5].

The universal character of the effective range function can be used to evaluate a very different system: low energy nucleon-deuteron scattering [6]. The effective range function corresponding to nucleon-deuteron scattering at low energies, in the $J = 1/2^+$ state, does not show the expected linear behavior but it presents a pole structure. First observations of this particular behavior have been done in Refs. [7, 8, 9] whereas in Ref. [10] explicit calculations of the effective range function have been done using nucleon-nucleon potentials. The pole structure has been related to a virtual state and, from the calculations, it was possible to extract the pole energy fitting the effective range formula with the form suggested by Delves [11]. Recently it was shown that the pole structure of the effective range function can be quantitatively related to the universal form given by equation (3) and, using the parametrization determined in the atomic three-helium system, that equation can be used to describe nucleon-deuteron scattering as well. In particular, using the universal function ϕ, the pole energy can be used to extract the three-body parameter κ_*. In this way, the universal behavior imposed by the DSI is analyzed in systems with natural lengths that differ of several order of magnitude.

The DSI imposes constrains also on the form of the S-matrix for energies above the dimer threshold. The following peculiar form for the recombination rate at threshold [12, 13] has been deduced:

$$K_3 = \frac{128\pi^2(4\pi - 3\sqrt{3})}{\sinh^2(\pi s_0) + \cosh^2(\pi s_0) \cot^2[s_0 \ln(\kappa_* a) + \gamma]} \frac{\hbar a^4}{m} \,, \tag{4}$$

and using the large value of the factor $e^{2\pi s_0} \approx 515$, the above equation can be approximated by

$$K_3 = \alpha\, a^4 \hbar/m \approx 67.1 \sin^2[s_0 \ln(\kappa_* a) + \gamma] a^4 \hbar/m \,, \tag{5}$$

where $\gamma = 1.16$ [5]. As it has been shown recently [14], this equation can be used to describe very different systems as recombination of three atoms or three nucleons.

The above discussion shows that the study of universality in few-body systems is of interest in several fields of research, ranging from cold-atoms to nuclear physics. In atomic physics, where the Efimov effect has been observed for the first time [15], discrepancies arise between the theoretical prediction and the experimental determination of the ratio between a_* and a_- [16, 17], that means between the scattering lengths at which the Efimov state disappears in the atom-dimer and in the three-atom continuum, respectively. The solution to this puzzle is probably hidden in finite-range corrections to the universal formulas (see Ref. [18] and references therein for a recent account to the problem). A recent study has discussed these corrections from a new perspective [19].

In nuclear physics these studies can be applied to describe halo nuclei where a cluster description is justified. We can mention the observation of universal aspects in the scattering of a neutron on a neutron-halo nucleus having a large scattering length, as for example the $n-^{19}$C system (see Refs. [20, 21] and Ref. [22] for a recent review). Also the light nuclei spectrum shows some universal characteristic as it has been discussed in Ref. [23].

2. The three-boson spectrum

The spectrum of the three-boson system (called trimer) having a large two-body scattering length a has been derived by Efimov in the zero-range limit [4]. The Efimov's binding energy equation is

$$E_3^n + \frac{\hbar^2}{ma^2} = \mathrm{e}^{-2(n-n^*)\pi/s_0} \exp\left[\Delta(\xi)/s_0\right] \frac{\hbar^2\kappa_*^2}{m}\,, \tag{6}$$

where $E_3^n/E_2 = \tan^2\xi$ and the function $\Delta(\xi)$ is an universal function defined in the range $-\pi \leq \xi \leq -\pi/4$ (a parametrization of $\Delta(\xi)$ in this range can be found in [5]). The two-body binding energy is defined in the zero-range limit as $E_2 = \hbar^2/ma^2$ and the three-body parameter κ_* is determined by the energy E_u^* of the n^* level at the unitary limit. The scattering length a appears as a control parameter, fixing its value the above equation has to be solved simultaneously with the condition $E_3^n/(\hbar^2/ma^2) = \tan^2\xi$ to find the the binding energies E_3^n at each value of the angle ξ. In this context the three-body parameter appears as a scale parameter. The universal character of the above equation can be seen using dimensionless quantities as

$$\epsilon^n = \mathrm{e}^{-2(n-n^*)\pi/s_0} \sin^2\xi \, \exp\left[\Delta(\xi)/s_0\right] \tag{7}$$

with $\epsilon_n = E_3^n/E_u^*$. This form of the equation explicitly shows DSI. At fixed values of the angle ξ the ratio between two different levels is constant and it results

$$E_3^n/E_3^{n'} = \mathrm{e}^{-2(n'-n)\pi/s_0}\,. \tag{8}$$

In the case of two consecutive levels the ratio $E_3^{n+1}/E_3^n = \mathrm{e}^{-2\pi/s_0} \approx 1/515.03$ is obtained. The behavior of the energy for two consecutive levels, $n = 0, 1$, as given in equation (7), is shown in figure 1. In order to see the two levels in a single plot the quantity $(\epsilon_n)^{1/4}$ is plotted as function of $\sqrt{x}$ with $x = \kappa_* a$. In the figure the following points are indicated: a_-^n and a_n^* are the values of the two-body scattering length at which the trimer disappears into the three-body continuum or into the atom-dimer continuum, respectively.

The Efimov equations are exact in the zero-range limit. They have been derived imposing a boundary condition in the short-range region encoded in the three-body parameter κ_*. The same problem has been studied using Effective Field Theories (EFT) [24]. In this approach the short-range physics enters through low energy constants, fitted to reproduce selected data. One particular form to apply this theory was suggested by Lepage [25]. The interaction between two

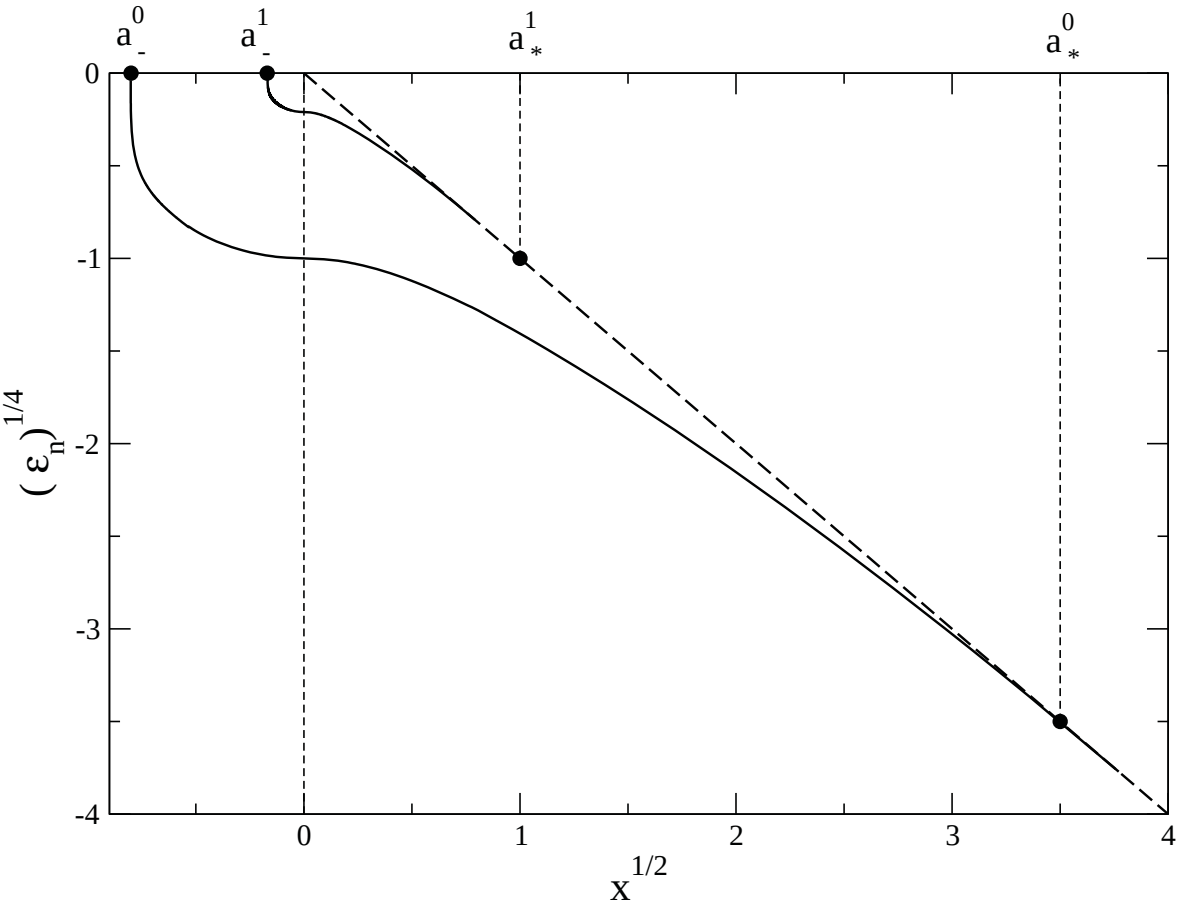

Figure 1. The dimensionless quantity $(\epsilon_n)^{1/4}$ as a function of $(x)^{1/2}$ for $n = 0, 1$. The particular values of the two-body scattering length a_-^n and a_*^n are indicated. The long-dashed line indicates the atom-dimer threshold.

particles is replaced by an effective potential parametrized in such a way that some relevant data are reproduced. For example, a two-parameter potential (as a gaussian) can be constructed to reproduce the scattering length and the effective range as given in equation (1). This effective interaction will describe the low energy dynamics of the system with good accuracy. The level of accuracy is given by the energy scale. Equation (1) is accurate at energies $E << E_0$, with $E_0 = \hbar^2/mr_0^2$, and errors in that formula appear at order of $(E/E_0)^2$. In the three-body system the leading order (LO) prescription of the EFT is that a three-body counter term has to be considered. At this order the EFT approach is based in a Hamiltonian with two coupling constants, one for the two body sector, related with the control parameter a, and one for the three-body sector, related to the scale parameter κ_*. The Efimov equations can be derived in this approach as has been shown if Ref. [26].

Following the above discussion, universal aspects of a three-boson system can be studied using a potential model. Following Refs. [6, 14, 27] the three-helium system is taken as a reference system. At the two-body level, one of the most commonly used He-He potentials, i.e., the LM2M2 interaction [28], is taken as the reference interaction. In particular, in order to explore the (a^{-1}, κ) plane ($\kappa = \text{sign}(E)[|E|/(\hbar^2/m)]^{1/2}$ and E the energy level), we modify this potential as:

$$V_\lambda(r) = \lambda V_{LM2M2}(r) \ . \tag{9}$$

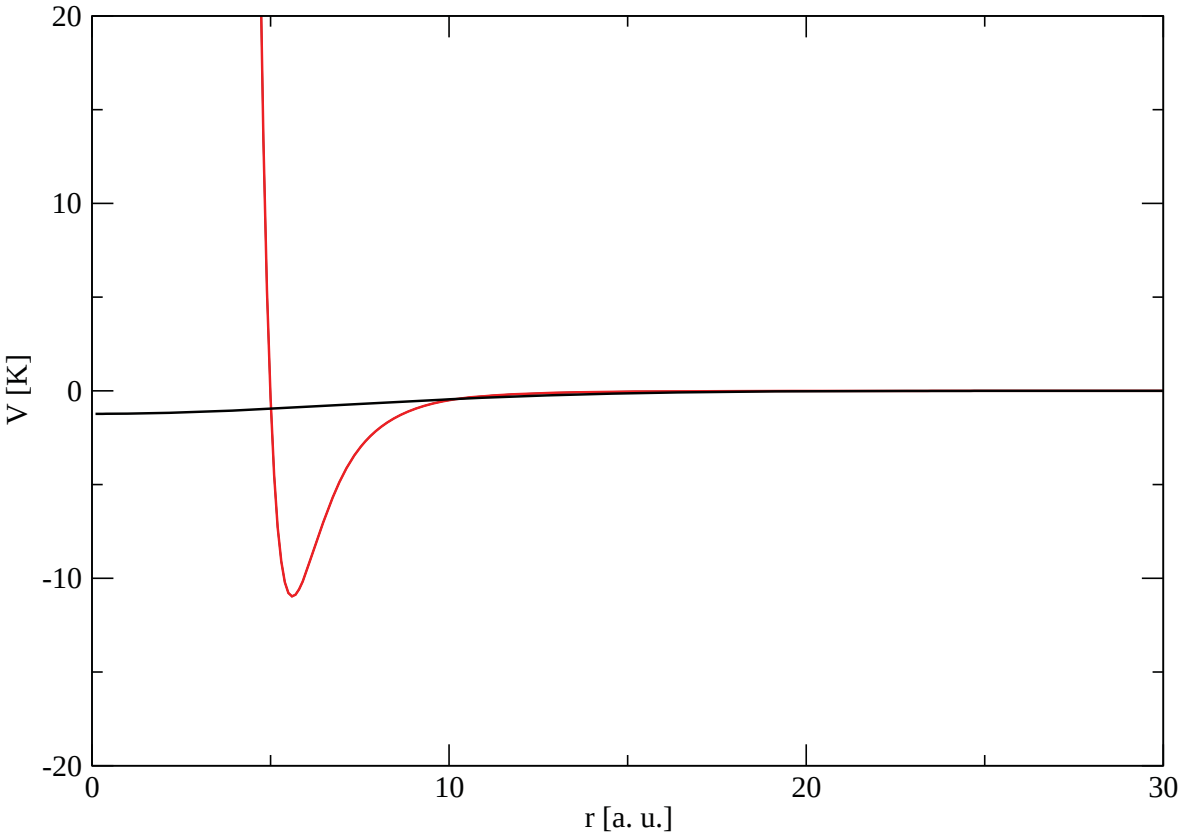

Figure 2. (Color online) The LM2M2 potential (red line) and the TBG potential (black line) as a function of the inter-particle distance.

Examples of this strategy exist in the literature [29, 30]. For $\lambda \approx 0.9743$ the interaction is close to the unitary limit ($a \to \infty$) and for $\lambda = 1$ the values predicted by the LM2M2 are recovered. The scattering length is $a = 189.41\ a_0$, the two-body energy $E_2 = -1.303$ mK and the effective range $r_s = 13.845\ a_0$, with the mass parameter $\hbar^2/m = 43.281307\,(a_0)^2$ K. Noticing the $r_0 \approx r_s$, the two-helium system has the $r_0/a << 1$ allowing a description based on the Efimov universal theory, having in mind that the range corrections have to be considered as well. As an effective potential we define an attractive two-body gaussian (TBG) potential [27, 31]

$$V(r) = V_0 \mathrm{e}^{-r^2/r_0^2} \tag{10}$$

with range $r_0 = 10\ a_0$ and strength V_0 fixed to reproduce the values of a given by $V_\lambda(r)$. For example with the strength $V_0 = -1.2343566$ K, corresponding to $\lambda = 1$, the LM2M2 low-energy data are closely reproduced, $E_2 = -1.303$ mK, $a = 189.42\ a_0$, and $r_s = 13.80\ a_0$. In figure 2 the two interactions are compared, the differences at short distanced are evident.

When the TBG potential is used in the three-atom system it produces a ground state binding energy appreciable deeper than that one calculated using the $V_\lambda(r)$ interaction. For example, at $\lambda = 1$ the LM2M2 helium-trimer ground-state binding energy is $E_3^0 = 126.4$ mK, whereas the one obtained using the TBG potential is 151.32 mK. Following the LO EFT prescription an hypercentral three-body (H3B) (repulsive) interaction can be introduced

$$W(\rho_{123}) = W_0 \mathrm{e}^{-\rho_{123}^2/\rho_0^2} \tag{11}$$

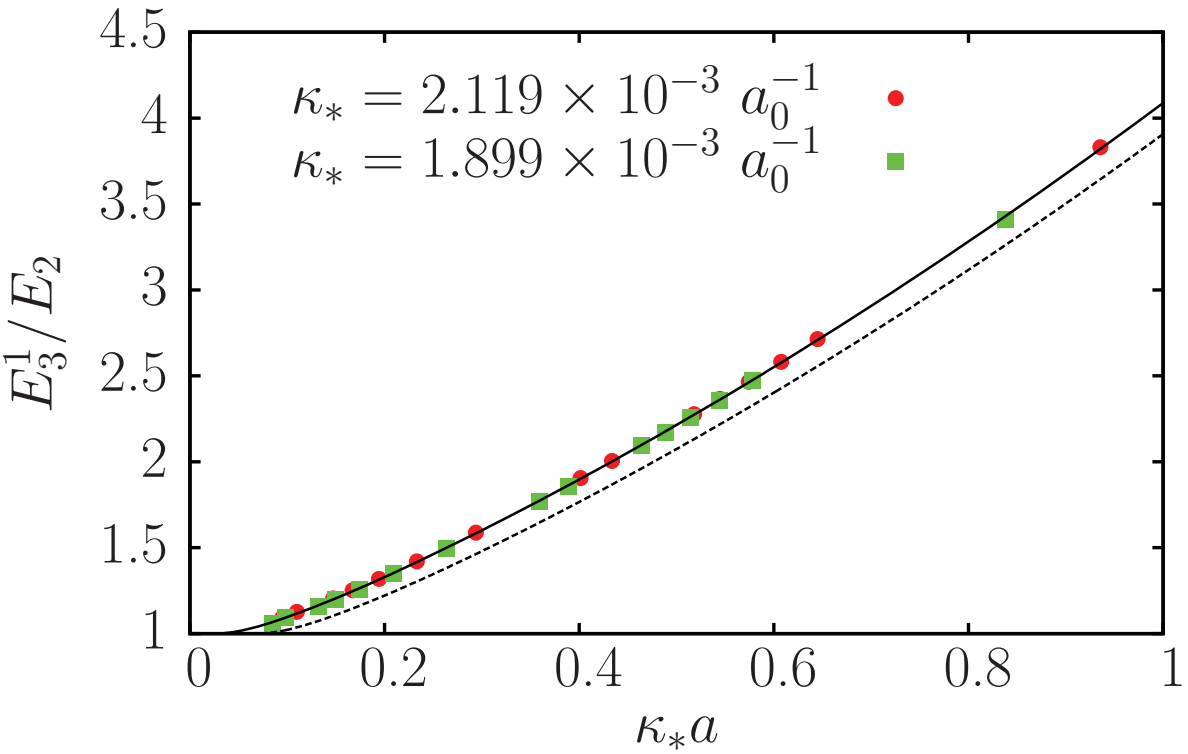

Figure 3. (Color online) The ratio between the excited state of the trimer and the dimer binding energy as a function of $\kappa_* a$ calculated for the TBG potential (red circles) and for the TBG+H3B potential (green squares). The dashed line represents the zero-range theory of equation (6) whereas the solid line has been obtained using equation (13).

with the strength W_0 tuned to reproduce the trimer E_3^0 obtained with $V_\lambda(r)$ for the different values of λ. In the above equation $\rho_{123}^2 = \frac{2}{3}(r_{12}^2 + r_{23}^2 + r_{31}^2)$ is the hyperradius of three identical particles and ρ_0 gives the range of the three-body force that can be fixed as $\rho_0 = r_0$.

Varying λ from the unitary limit to $\lambda = 1.1$ a set of values for the ground state binding energy E_3^0 and the first excited state E_3^1 using the TBG and TBG+H3B potentials can be obtained in a broad range of a. The results can be compared to the predictions given by the Efimov's binding energy equation. Fixing $n^* = 1$, the three-body parameter κ_* is determined by calculating E_3^1 at the unitary limit; we obtain $\kappa_* = 2.119 \times 10^{-3}\, a_0^{-1}$ and $\kappa_* = 1.899 \times 10^{-3}\, a_0^{-1}$ for the TBG and TBG+H3B, respectively.

As it has been shown in Refs. [6, 14, 19], in order to be in accord with the numerical results obtained solving a finite-range potential, the universal relation equation (6) must be modified in the following way

$$E_3^n/E_2 = \tan^2\xi \tag{12}$$

$$\kappa_* a + \Gamma_n = \mathrm{e}^{(n-n^*)\pi/s_0} \exp\left[-\Delta(\xi)/2s_0\right]/\cos\xi\,. \tag{13}$$

The finite-range nature of the interaction has been taken into account by the substitution $\hbar^2/ma^2 \to E_2$ in the first row. The main modification however is the introduction of the shift Γ_n. In figure 3 we collect our numerical results for the ratio E_3^1/E_2 as a function of $\kappa_* a$ for the TBG potential (circles) and for the TBG+H3B potential (squares). The dashed line corresponds to the zero-range theory given in equation (6), whereas the solid line, which goes on top of the numerical results, has been obtained using equation (13) with $\Gamma_1 \approx 4 \times 10^{-2}$.

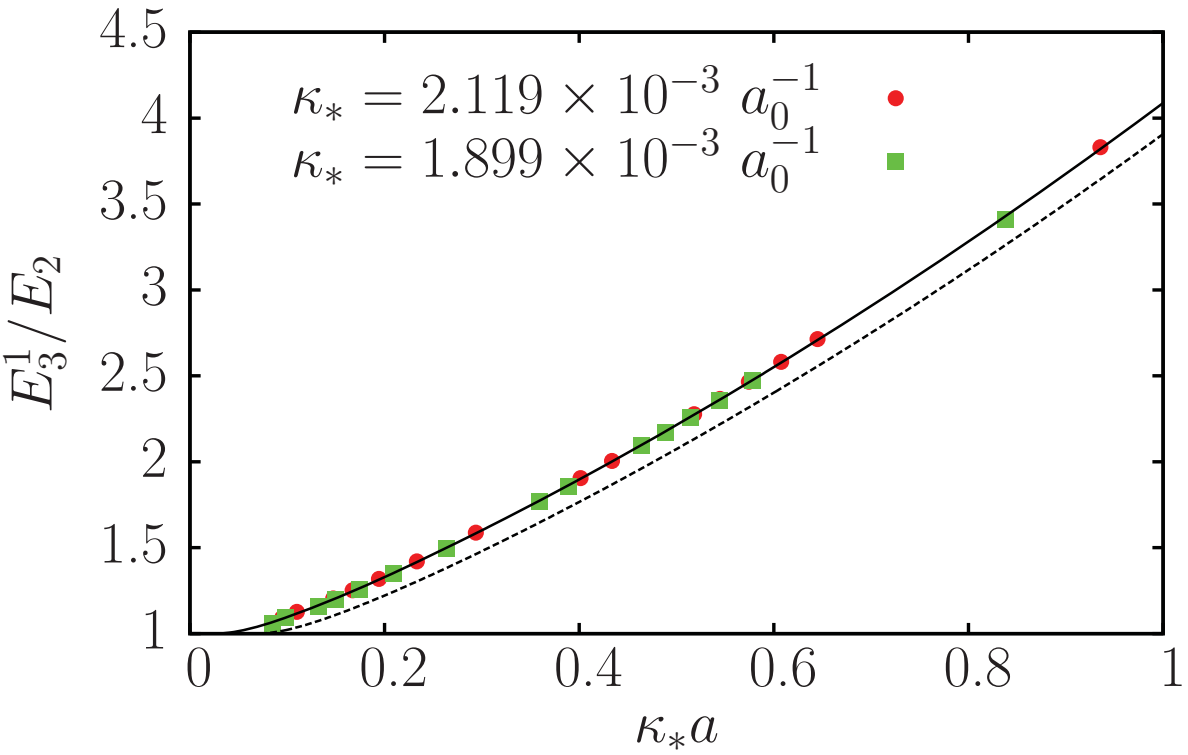

Figure 4. (Color online) The atom-dimer scattering length a_{AD} in units of a_B calculated for the TBG (red circles) and TBG+H3B (green squares) potentials. The dashed line represents the zero-range theory of equation (2) whereas the solid and dotted line are the finite-range theory of equation (14). In the latter a slightly different parametrization of the constants d_1, d_2 and d_3 is used.

3. Atom-dimer scattering

The effective potential models, TBG and TBG+H3B, described in the previous section can be used to describe atom-dimer scattering and the recombination rate K_3 at threshold. To this end the dimer-atom scattering length a_{AD} and the s-wave atom-dimer phase δ can be calculated. The calculations have been done using the hyperspherical harmonic (HH) method as described in Refs. [31, 32]. The results for the atom-dimer scattering length are collected in figure 4 where the ratio a_{AD}/a_B is given in terms of the product $\kappa_* a$ (the energy scattering length a_B is defined from the dimer binding energy as $E_2 = \hbar^2/m a_B^2$). It can be observed that the calculated points, given as full circles (TBG potential) and full squares (TBG+H3B potential), are on a curve shifted with respect to the dashed line representing the zero-range theory of equation (2) with the parametrization given in Ref. [5]. We can interpret again the shift as produced by the finite-range character of the calculations. Accordingly equation (2) can be modified to describe finite-range interactions as

$$a_{AD}/a_B = d_1 + d_2 \tan[s_0 \ln(\kappa_* a + \Gamma_*) + d_3] \ , \tag{14}$$

Using the values $\Gamma_* = \Gamma_1$, the solid line is obtained in figure 4. Furthermore, modifying slightly the values of the universal constants as $d_1 = 1.531$, $d_2 = -2.141$ and $d_3 = 1.100$, from those given in Ref. [5], a better description of the numerical results is obtained as it is shown by the dotted line in the figure.

The calculations have been extended to describe atom-dimer scattering at energies below the dimer breakup threshold for different values of a. As it has been done for the zero-range theory

of the binding energies and atom-dimer scattering length, equation (3) has to be modified to consider finite-range interactions. Following Ref. [6], the effective range function can be written as

$$ka_B \cot\delta = c_1(ka) + c_2(ka)\cot[s_0 \ln(\kappa_* a + \Gamma_*) + \phi(ka)] \ . \tag{15}$$

The results are collected in figure 5 (full squares) at different values of $\kappa'_* a = \kappa_* a + \Gamma_*$. In the figure different patterns can be observed. For the smallest values of $\kappa'_* a$ the behavior is almost linear in all the energy range. Starting at values $\kappa'_* a \approx 0.4$ a curvature appears close to zero energy, pointing out to an emergent pole structure that becomes evident at larger values of $\kappa'_* a$. Specifically, the pole appears when a_{AD} changes sign (see figure 4) or when the argument of the cotangent function in equation (15) becomes zero (or $n\pi$). The shadow plot in the first row of figure 5 corresponds to the case $\lambda = 1$ and describes ^{4}He-^{4}He$_2$ scattering (full triangles). The shadow plot in the second row corresponds to nucleon-deuteron scattering as discussed below. The solid curves are obtained using the finite-range theory of equation (15) with the parametrization of Ref. [5]. We can observe a noticeable agreement along the whole range of values.

The effective range function in the case of neutron-deuteron scattering has a peculiar form [10]. Moreover Efimov claimed that this process can be described with the universal formula of equation (3) [4]. In order to verify this property, equation (15) can be applied to quantitatively describe $n-d$ scattering at low energies. To this end the results of Ref. [10], in which $n-d$ scattering has been described using a spin dependent central potential, can be used. In that reference the value of $a_{nd} = 0.71\,\text{fm}$ has been obtained for the $n-d$ scattering length, and the effective range function has been parametrized as

$$k\cot\delta = \frac{-1/a_{nd} + r_s k^2/2}{1 + E_{c.m.}/E_p} \tag{16}$$

with $E_p = -160$ keV and $r_s \approx -127\,\text{fm}$. It should be noticed that this particular parametrization of the effective range function can be simple related to equation (15) in the low energy limit. From the values of E_p and a_{nd} it is possible to determine the values of a and κ'_* using the universal function ϕ and equation (14). The values $a = 4.075\,\text{fm}$ and $\kappa'_* a = 0.5779$ are obtained. The negative energy E_p of the pole implies that it appears in the negative region similar to what happens in figure 5 at intermediate $\kappa'_* a$ values. With these numerical values the shadow panel of the second row in figure 5 shows a comparison between equation (15) and the $n-d$ scattering results of Ref. [10] (full circles). A noticeable agreement is observed. Is should be stressed that the universal functions used in equation (15) are those obtained through the analysis of the atomic system.

Finally the application of the finite-range theory is discussed in the case of the recombination rate at threshold corresponding, in the case of three-helium atoms, to the process ^{4}He+^{4}He+^{4}He $\rightarrow$ ^{4}He+^{4}He$_2$. The coefficient can be defined as $K_3 = \alpha(\hbar a^4/m)$. The DSI imposes α to be a log-periodic function, as given in equation (4), whose simplified version is given in equation (5). In order to describe the numerical results obtained using finite-range potentials, the following modification in the definition of K_3 has to be introduced

$$K_3 = \frac{128\pi^2(4\pi - 3\sqrt{3})}{\sinh^2(\pi s_0) + \cosh^2(\pi s_0)\cot^2[s_0 \ln(\kappa_* a + \Gamma_+) + \gamma]} \frac{\hbar a_B^4}{m} \,, \tag{17}$$

with the simplified form

$$K_3 = \alpha\, a^4 \hbar/m \approx 67.1 \sin^2[s_0 \ln(\kappa_* a + \Gamma_+) + \gamma] a_B^4 \hbar/m \,, \tag{18}$$

where, as in the effective range function, a has been replaced by a_B and the shift Γ_+ has been introduced. The results obtained in Ref. [14] are shown in figure 6 as circles (TBG potential)

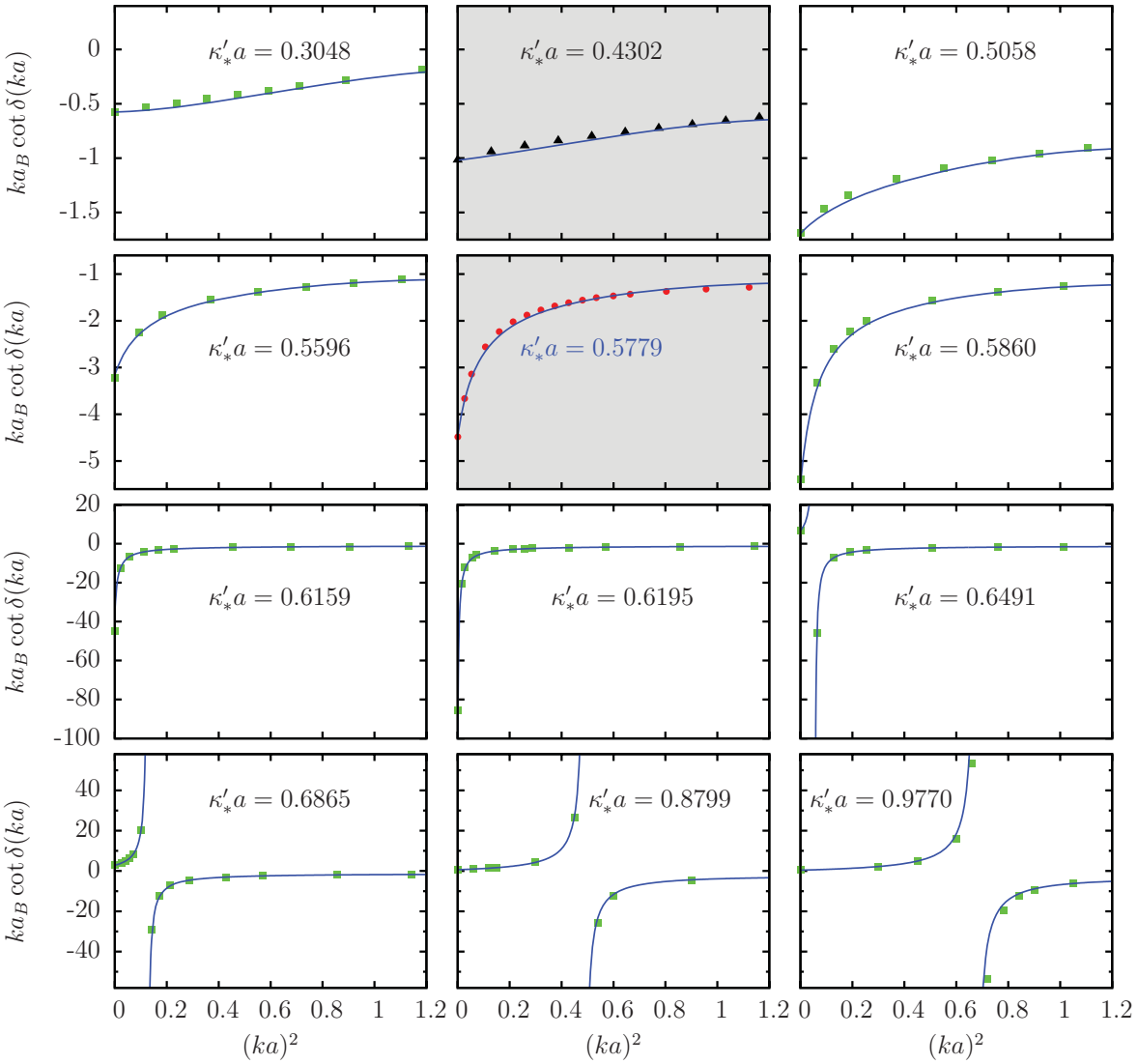

Figure 5. (Color online) The effective range function (squares) at different values of $\kappa'_* a$ as a function of $(ka)^2$. The triangle points are the calculations for real ^{4}He-^{4}He$_2$ scattering. The full circles, for $\kappa'_* a = 0.5779$, correspond to neutron-deuteron scattering in the doublet channel. The solid curves have been calculated using equation (15) for different values of $\kappa'_* a$.

and squares (TBG+H3B potential). The dashed line represents equation (4) using the value $\gamma = 1.16$ from Ref. [5]. From the figure it is evident that the calculated points organize in a curve shifted with respect to the universal curve. The solid line represents equation (17), with the same value of γ and $\Gamma_+ \approx 6 \times 10^{-2}$. Again the finite-range theory obtained by modifying the zero-range equations with a shift in the variable $\kappa_* a$ describes the calculated points with good accuracy. Moreover the values of the shifts Γ_1, Γ_* and Γ_+ are of the same order.

4. Light nuclei spectrum

In this section the spectrum obtained for $N \leq 6$ fermions is discussed using a central potential. The intention here is to see if, in the case of fermions, some of the universal properties discussed

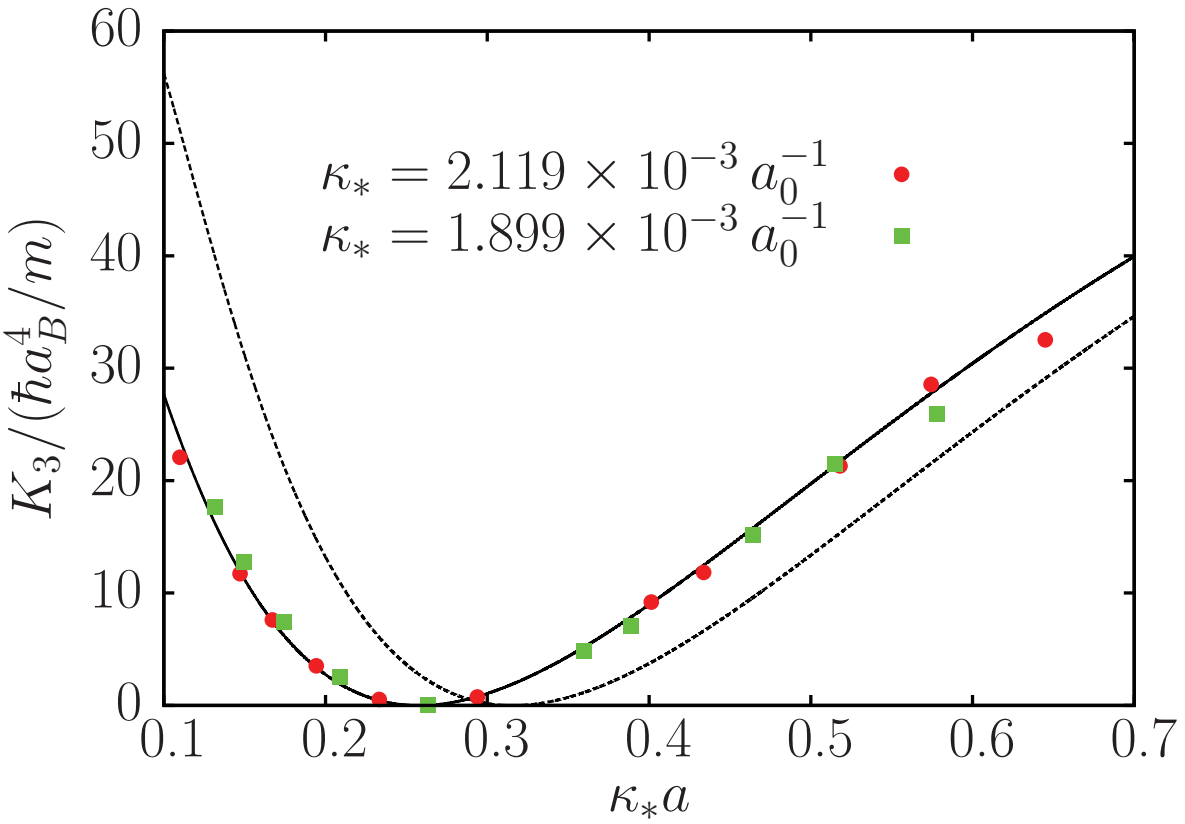

Figure 6. (Color online) The recombination rate K_3 at threshold for different values of $\kappa_* a$ calculated for the TBG (red circles) and TBG+H3B (green squares) potentials. The dotted line is the zero-range theory of equation (4) whereas the solid line is the finite-range theory of equation (17).

before can be identified in the spectrum of light nuclei. To this end the following central potential, the Volkov potential,

$$V(r) = V_R \mathrm{e}^{-r^2/R_1^2} + V_A \mathrm{e}^{-r^2/R_2^2} \tag{19}$$

is used with $V_R = 144.86\,\mathrm{MeV}$, $R_1 = 0.82\,\mathrm{fm}$, $V_A = -83.34\,\mathrm{MeV}$, $R_2 = 1.60\,\mathrm{fm}$. The fermions are considered to have the same mass, chosen to be equal to the reference mass m, and corresponding to $\hbar^2/m = 41.47\,\mathrm{MeV\ fm^2}$ (nuclear case). With this parametrization of the potential, the two-nucleon system has binding energy $E_2 = 0.54592$ MeV and scattering length $a = 10.082\,\mathrm{fm}$. For $N > 2$ the use of the s-wave version of the potential produces a spectrum much closer to the experimental one. This is a direct consequence of the weakness of the nuclear interaction in p-waves. The results are obtained after diagonalizing the Hamiltonian matrix constructed using the HH basis without symmetrization as discussed in Ref. [23].

With the parametrization of the potential given above, the ^{3}H and ^{3}He binding energies result to be 8.431 MeV and 7.725 MeV, very close to the experimental values. In fact, this parametrization was chosen to correctly describe the three-nucleon binding energies and, for this reason, the deuteron binding energy results artificially low. As a consequence ^{3}H has an excited state close to the nucleon-deuteron threshold. Using a more realistic interaction this state should move above the threshold becoming the virtual state discussed in the previous section. In despite of its simplicity this model predicts the ^{4}He binding energy with an error

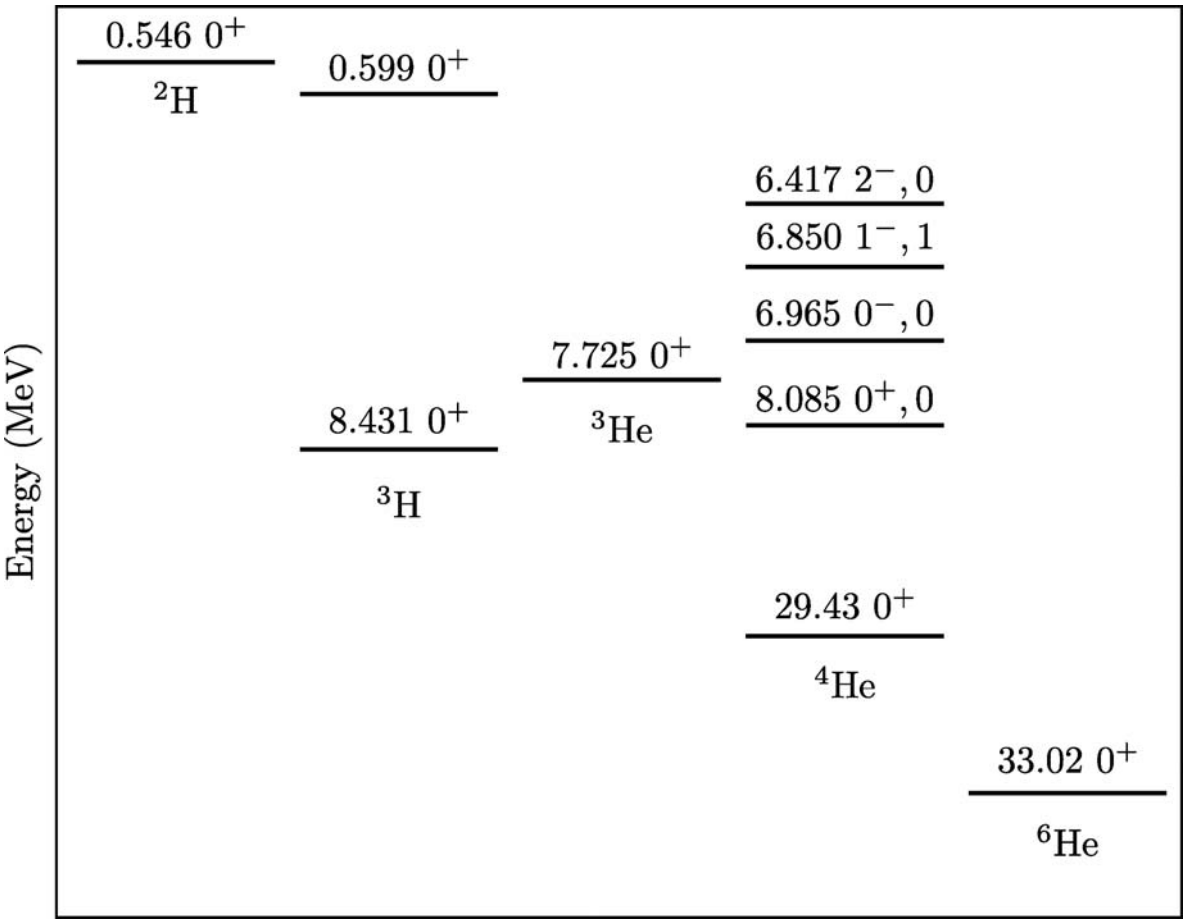

Figure 7. Calculated levels for $A = 2, 3, 4$ and 6, using the Volkov potential with the inclusion of the Coulomb interaction for the He isotopes.

below 5% and, more interesting, the almost correct position of the 0^+ excited state, as is shown in figure 7. Without considering the spin-dependence of the force the ^{6}He ground state energy results too bound.

5. Conclusions

The zero-range theory for few-body systems having a large two-body scattering length a has been studied and discussed using potential models. Following the prescription of Lepage [25] an effective interaction has been constructed that reproduces the same low energy data: the two-body scattering a, acting as a control parameter, and the energy wave number κ_* of one selected level of the trimer at the unitary limit, acting as a scale parameter. Using this model different observables have been calculated solving the Schrödinger equation: the three-boson energy spectrum, the atom-dimer scattering length, the atom-dimer effective range function and the recombination rate at threshold. The analysis of the numerical results allowed to judge the capability of the zero-range theory to describe finite-range systems. The conclusion was that a finite-range scale parameter Γ_n has to be introduced to correct the original zero-range theory. This parameter appears as a finite-range scaling parameter.

Using the finite-range theory it was possible to describe very different systems as atom-dimer scattering and neutron-deuteron scattering using the same parametrization of the universal

effective range function, equation (15), obtained studying atomic systems. As a final study, the spectrum of light nuclear systems has been analyzed using a central potential, the Volkov potential. Fixing only the ^{3}H binding energy, this simple model describes the binding energies of the ground and excited states in ^{4}He with an error below 5%. The ^{6}He results slightly over bind. Studies including the spin dependence of the interaction are at present underway.

References

[1] Thomas L H 1935 *Phys. Rev.* **47** 903
[2] Efimov V 1970 *Phys. Lett. B* **33** 563
[3] Efimov V 1971 *Sov. J. Nucl.* **12** 589
[4] Efimov V 1979 *Sov. J. Nucl.* **29** 546
[5] Braaten E and Hammer H W 2006 *Phys. Rep.* **428** 259
[6] Kievsky A and Gattobigio M 2013 *Phys. Rev. A* **87** 052719
[7] Barton G and Phillips A 1969 *Nucl. Phys. A* **132** 97
[8] Whiting J S and Fuda M G 1976 *Phys. Rev. C* **14** 18
[9] Girard B A and Fuda M G 1979 *Phys. Rev. C* **19** 579
[10] Chen C R, Payne G L, Friar J L, and Gibson B F 1989 *Phys. Rev. C* **39** 1261
[11] Delves L M 1960 *Phys. Rev.* **118** 1318
[12] Nielse E and Macek J H 1999 *Phys. Rev. Lett.* **83** 1566
[13] Esry B D, Greene C H, and Burke J P 1999 *Phys. Rev. Lett.* **83** 1751
[14] Garrido E, Gattobigio M, and Kievsky A 2013 *Phys. Rev. A* **88** 032701
[15] Kraemer T *et al.* 2006 *Nature* **440** 315
[16] Zaccanti M *et al.* 2009 *Nat. Phys.* **5** 586
[17] Machtey O, Shotan Z, Gross N, and Khaykovich L 2012 *Phys. Rev. Lett.* **108** 210406
[18] Dyke P, Pollack S E, and Hulet R G 2013 *Phys. Rev. A* **88** 023625
[19] Gattobigio M and Kievsky A 2014 `arXiv:1309.1927`
[20] Mazumdar I, Rau A R P, and Bhasin V S 2006 *Phys. Rev. Lett.* **97** 062503
[21] Yamashita M, Frederico T, and Tomio L 2008 *Phys. Lett. B* **670** 49
[22] Frederico T, Delfino A, Tomio L, and Yamashita M 2012 *Prog. Part. Nucl. Phys.* **67** 939
[23] Gattobigio M, Kievsky A, and Viviani M 2011 *Phys. Rev. C* **83** 024001
[24] Bedaque P F, Hammer H W, and van Kolck U 1999 *Phys. Rev. Lett.* **82** 463
[25] Lepage G P 1999 *Particles and fields* eds Barata J C A, Malbouisson A P C, and Novaes S F (Singapore: World Scientific)
[26] Bedaque P F, Hammer H W, and van Kolck U 1999 *Nucl Phys. A* **646** 444
[27] Gattobigio M, Kievsky A, and Viviani M 2012 *Phys. Rev. A* **86** 042513
[28] Aziz R A and Slaman M J 1991 *J. Chem. Phys.* **94** 8047
[29] Esry B D, Lin C D, and Greene C H 1996 *Phys. Rev. A* **54** 394
[30] Barletta P and Kievsky A 2001 *Phys. Rev. A* **64** 042514
[31] Kievsky A, Garrido E, Romero-Redondo C, and Barletta P 2011 *Few-Body Syst.* **51** 259
[32] Kievsky A 1997 *Nucl. Phys. A* **624** 125